



Published in final edited form as:

J Neurochem. 2009 September ; 110(5): 1648–1660. doi:10.1111/j.1471-4159.2009.06262.x.

INSULIN RECEPTOR SIGNALING REGULATES ACTIN CYTOSKELETAL ORGANIZATION IN DEVELOPING PHOTORECEPTORS

Raju V.S. Rajala^{1,2,3}, Ammaji Rajala^{1,3}, Richard S. Brush^{1,3}, Nora P. Rotstein⁴, and Luis E. Politi⁴

¹ Department of Ophthalmology, University of Oklahoma Health Sciences Center, Oklahoma City, Oklahoma

² Department of Cell Biology, University of Oklahoma Health Sciences Center, Oklahoma City, Oklahoma

³ Dean A. McGee Eye Institute, University of Oklahoma Health Sciences Center, Oklahoma City, Oklahoma

⁴ Instituto de Investigaciones Bioquimicas (INIBIBB), CONICET and Universidad Nacional del Sur, Bahia Blanca, Argentina

Abstract

The insulin receptor (IR) and IR signaling proteins are widely distributed throughout the central nervous system. IR signaling provides a trophic signal for transformed retinal neurons in culture and we recently reported that deletion of IR in rod photoreceptors by *Cre/lox* system resulted in stress-induced photoreceptor degeneration. These studies suggest a neuroprotective role of IR in rod photoreceptor cell function. However, there are no studies available on the role of insulin-induced IR signaling in the development of normal photoreceptors. To examine the role of insulin-induced IR signaling, we analyzed cultured neuronal cells isolated from newborn rodent retinas. In insulin-lacking cultures, photoreceptors from wild type rat retinas exhibited an abnormal morphology with a wide axon cone and disorganization of the actin and tubulin cytoskeleton. Photoreceptors from IR knockout mouse retinas also exhibited a similar abnormal morphology. A novel finding in this study was that addition of docosahexaenoic acid (DHA), a photoreceptor trophic factor, restored normal axonal outgrowth in insulin-lacking cultures. These data suggest that IR-signaling pathways regulate actin and tubulin cytoskeletal organization in photoreceptors; they also imply that insulin and DHA activate at least partially overlapping signaling pathways that are essential for the development of normal photoreceptors.

Keywords

Insulin; Insulin Receptors; Retina; docosahexaenoic acid; differentiation; photoreceptors; neurite outgrowth; neuron survival

INTRODUCTION

The insulin receptor (IR) is a transmembrane receptor that is activated by insulin. It belongs to the large class of tyrosine kinase receptors. It induces cellular responses by

phosphorylating proteins on tyrosine residues. The IR and IR-signaling proteins are widely distributed throughout the central nervous system (Havrankova et al. 1978). IR signaling regulates food intake (Baskin et al. 1999; Schwartz et al. 1992) and neuronal growth and differentiation (Heidenreich 1993; Robinson et al. 1994).

IR activation has been shown to rescue retinal neurons from apoptosis through a phosphoinositide 3-kinase (PI3K) cascade (Barber et al. 2001). We previously reported that light induces tyrosine phosphorylation of the retinal IR and that this activation leads to the binding of PI3K to rod outer segment (ROS) membranes (Rajala et al. 2002). More recently, we demonstrated that IR activation is mediated through the G-protein-coupled receptor, rhodopsin (Rajala et al. 2007). IR signaling is also involved in 17 β -estradiol-mediated neuroprotection in the retina (Yu et al. 2004). Recent evidence suggests a down regulation of IR kinase activity in diabetic retinopathy that is associated with the deregulation of downstream signaling molecules (Reiter et al. 2006). Deletion of several downstream effector molecules of the IR signaling pathway in the retina, such as IRS-2 (Yi et al. 2005), Akt2 (Li et al. 2007), and bcl-xl (Zheng et al. 2006), resulted in photoreceptor degeneration. We used the Cre/lox system to specifically inactivate the IR gene in rod photoreceptors (Rajala et al. 2008). Reduced IR expression in rod photoreceptors significantly decreased retinal function and caused the loss of photoreceptors in mice exposed to bright light stress (Rajala et al. 2008). These studies clearly indicate the importance of the IR signaling pathway in the retina.

The IR is highly conserved and the high degree of IR signaling homology between *C. elegans*, *Drosophila*, and humans suggests functional conservation in the mammalian retina. The IR regulates neuronal survival in *C. elegans* (Wolkow et al. 2000). In *Drosophila*, the IR serves the important function of guiding retinal photoreceptor axons from the retina to the brain during development (Song et al. 2003) and the IR influences the size and number of photoreceptors (Brogiolo et al. 2001). Lack of IR activation leads to neurodegeneration in brain/neuron-specific IR knock-out mice (Schubert et al. 2004). Dysregulation of insulin signaling in the CNS has been linked to the pathogenesis of neurodegenerative disorders such as Alzheimer's and Parkinson's diseases (Takahashi et al. 1996; Frolich et al. 1998). These studies clearly suggest that the IR pathway is important for neuronal survival and maintenance.

Studies from our laboratory (Rajala et al. 2008) and others (Barber et al. 2001) suggest that IR signaling is important for neuron survival in the retina and down regulation of this pathway is one of the contributory factors in diabetic retinopathy (Reiter et al. 2006). However, there are no studies available on the role of IR in photoreceptor differentiation. In this study we examined the role of IR signaling in normal photoreceptor differentiation. Studies were conducted on rodent retinal neurons cultured in a chemically-defined medium (Politi et al. 1988) which differentiated into photoreceptor and amacrine neurons (Rotstein et al. 1996). In insulin-lacking cultures, photoreceptors from wild type rat retinas exhibited an abnormal morphology with a wide axon cone and disorganization of the actin and tubulin cytoskeleton. Photoreceptors lacking insulin receptors also exhibited a similar abnormal morphology. These results indicate that the IR regulates the cytoskeletal organization in rod photoreceptors. A novel finding in this study was that addition of DHA, a photoreceptor trophic factor, restored normal axonal outgrowth in insulin-lacking cultures. These data suggest that IR-signaling pathways regulate actin and tubulin cytoskeletal organization in photoreceptors; they also imply that insulin and DHA activate at least partially overlapping signaling pathways that are essential for the regulation of actin cytoskeletal organization in developing photoreceptors.

EXPERIMENTAL PROCEDURES

Materials

Polyclonal anti-IR β and anti-tubulin antibodies were obtained from Santa Cruz Biotechnology (Santa Cruz, CA). Anti-opsin (R1D4) antibody was a kind gift from Dr. Robert Molday, University of British Columbia, Vancouver, Canada. Actin antibody was obtained from Affinity BioReagents (Golden, CO). Monoclonal anti-acetylated α -tubulin antibody was from Sigma Chemical Co. (St. Louis, MO). Rhodamine-labeled phalloidin was from Molecular Probes, Invitrogen. Secondary antibody, Cy2-conjugated goat anti-rabbit was from Jackson ImmunoResearch (West Grove, PA). Cytochalasin was from Calbiochem (San Diego, CA). All other reagents were of analytical grade and from Sigma (St. Louis, MO).

Animals

All animal work was in strict accordance with the *NIH Guide for the Care and Use of Laboratory Animals* and the Association for Research in Vision and Ophthalmology on the Use of Animals in Vision Research. All protocols were approved by the IACUC at the University of Oklahoma Health Sciences Center and the Dean McGee Eye Institute. Sprague-Dawley (Harlan Sera-Lab; Indianapolis, Indiana) rats were born and raised in our vivarium, and kept under dim cyclic light (5 lux, 12h on/off, 7AM–7PM) prior to experimentation. Photoreceptor-specific conditional insulin receptor knockout mice (Rajala et al. 2008) were born in 60 lux cyclic light (12h on/off) in the animal facility and maintained under these lighting conditions.

Generation of Photoreceptor-Specific IR Knockout Mice

The generation of photoreceptor-specific IR knockout mice has been described previously (Rajala et al. 2008). The genotype of the photoreceptor-specific IR knockout mice (i.e., animals carrying the *cre* transgene and homozygous for the IR floxed allele) was confirmed by PCR analysis of tail DNA. To identify rhodopsin-*cre*, PCR was performed with 1 μ l of genomic DNA and sense (5'-GGT CAG TGC CTG GAG TTG CG-3') and antisense (5'-GCC TCC ACC CGA TGT CAC C-3') primers to amplify a 600-bp product. To identify IR-floxed mice, we used sense (5'-GAT GTG CAC CCC ATG TCT G-3') and antisense (5'-CTG AAT AGC TGA GAC CAC AG-3') primers to amplify genomic DNA by PCR. The wild-type allele generates a 280-bp product, and the floxed allele generates a 300-bp product.

Immunolabeling of ROS and Whole Mount Preparations

Intact ROS, some containing blebs of inner segments attached through the connecting cilium, were prepared by mechanical detachment from freshly dissected bovine retinas as a suspension in Hanks' balanced salt solution (Sigma Chemical Co, St. Louis, MO) buffered with 25 mM HEPES (pH 7.4)(Muresan et al. 1993). After gentle homogenization by five passes through a Pasteur pipette, cell fragments in suspension were allowed to adsorb for 3 min to a VectabondTM (Vector Laboratories, Burlingame, CA)-treated glass slide. Adhered cell fragments were fixed for 5 min in methanol at -20°C and washed 3 times with PBS before processing for immunostaining. To detect IR in the dissociated photoreceptors, slides were incubated with anti-IR β with a dilution of 1:1000 in PBS containing 10% horse serum. The photoreceptor identity was verified by mouse anti-opsin (1:100) antibody. Antibodies were incubated overnight at 4°C and washed with PBS. For fluorescent detection, slides were incubated with Texas-red-anti-mouse antibody (Vector Laboratories), diluted 1:200 in PBS with 10% horse serum. Following incubation for 1h at room temperature, the slides were washed with PBS and cover-slipped in 50% glycerol in PBS. Antibody-labeled

complexes were examined on a Nikon Eclipse E800 microscope equipped with a digital camera and images were captured using Metamorph (Universal Imaging, West Chester, PA) image analysis software. For quantitation, all images were captured using identical microscope and camera settings so that intensities of the digital images quantitatively reflect antibody binding.

Preparation of Mouse Rod Outer Segments

Light- (LROS) and dark-adapted (DROS) ROS were prepared according to the method described earlier (Rajala et al. 2002). ROS were prepared from mouse retinas using discontinuous sucrose gradient centrifugation as previously described (Rajala et al. 2007). Eight retinas from 4 mice were homogenized in 1.25 ml of ice-cold 47% sucrose solution containing 100 mM NaCl, 1 mM EDTA, 1 mM phenylmethylsulfonyl fluoride (PMSF), and 10 mM Tris-HCl (pH 7.4). Retinal homogenates were transferred to 4.5-ml centrifuge tubes and sequentially overlaid with 1.5 ml of 37%, then 1.0 ml of 32% sucrose dissolved in buffer A. The gradients were spun at $82,000 \times g$ for 1 h at 4 °C. The 32%/37% interfacial sucrose band containing ROS membranes was harvested and diluted with 10 mM Tris-HCl (pH 7.4) containing 100 mM NaCl, and 1 mM EDTA, and centrifuged at $27,000 \times g$ for 30 min. The ROS pellets were resuspended in 10 mM Tris-HCl (pH 7.4) containing 100 mM NaCl and 1 mM EDTA and stored at -20 °C. Protein concentrations were determined by using the BCA reagent from Pierce (Pierce, Rockford, IL) following the manufacturer's instructions.

Neuroretina Cultures

Experiments were conducted with wild type and IR knockout mice or with albino Wistar rats. Primary cultures of retinal neurons were prepared from 2 to 4 day-old pups by the trypsinization-dissociation technique as described by Politi et al. (Politi et al. 1996; Politi et al. 1988). In brief, dissected retinas were incubated 12–13 min with 0.125% trypsin in Ca^{2+} , Mg^{2+} -free Hank's balanced salt solution, sequentially rinsed with trypsin inhibitor and mechanically dissociated with a 5-ml glass pipette. Cells were resuspended in culture medium and seeded in 35-mm plastic dishes (Corning) previously precoated overnight with polyornithine (50 $\mu\text{g}/\text{ml}$ in borate buffer, pH 8.4) followed by a 20% Schwannoma-conditioned medium containing neurite-promoting factor (Adler 1982) in a Dulbecco's modified Eagles medium (DME). Cells were incubated in a serum- and lipid-free chemically defined medium consisting of DME supplemented with gentamicin (50 mg/L), glutamine (2 mM), cytidine 5-diphosphocholine (2.56 mg/L), cytidine 5-diphosphoethanolamine (1.28 mg/L), hydrocortisone (100 nM), insulin (1.66 μM), progesterone (4×10^{-8} M), putrescine (2×10^{-4} M), selenium (6×10^{-8} M), glucose (5.6 mM) and transferrin (12.5×10^{-8} M) as reported by Politi et al. (Politi et al. 1988).

To evaluate the effect of insulin deficiency in neurons from normal retinas, neuronal cultures were prepared and incubated in insulin-lacking cultures. To investigate the effect of high glucose and high insulin on neuronal development, cultures were supplemented with 25 mM glucose and 16.6 μM insulin, respectively. The effect of DHA, a photoreceptor survival factor (Rotstein et al. 1996; Rotstein et al. 1997; German et al. 2006), was investigated in cultures with or without insulin. DHA (6.7 μM) was added to day-1 cultures, complexed with bovine serum albumin (BSA) in a 2:1 molar ratio. The same volume and concentration of a BSA solution was simultaneously added to control cultures.

Retinal cultures were incubated for different periods at 36 °C in a humidified atmosphere of 5% CO_2 in air. The identification of different neurons was based on (1) morphological criteria, by using phase-contrast microscopy, and (2) the differential expression of opsin and

other cell-specific antigens, detected by immunocytochemical methods with specific monoclonal antibodies.

Cytochalasin Treatment

Cytochalasin D (2 μ M in dimethylsulfoxide, DMSO) was added to cultures with or without insulin, and with or without DHA at day 3. Cells were fixed 30 min later.

Immunocytochemical Methods

Cells were fixed for at least 1 hour with 2% paraformaldehyde in PBS at room temperature, followed by permeation with Triton X-100 (0.1 % in PBS) for 15 minutes. Amacrine cells were identified with the anti-syntaxin monoclonal antibody, HPC-1. Cy2-conjugated-goat anti-mouse was used as the secondary antibody. To visualize the actin cytoskeleton, cells were incubated with Rhodamine-labeled phalloidin for 20 min. Expression of acetylated α -tubulin was determined by immunocytochemistry.

Cultures were then analyzed by phase and fluorescence microscopy using a Nikon Eclipse E600 microscope with a C-C Phase Contrast Turrent Condenser and a Y-FL Epi-Fluorescence Attachment and by a Laser Scanning Confocal Microscope (LSCM; Leica DMIRE2/TSCSP2) with a 63 water objective. x - y (top to bottom); sections were collected and processed with LCS software (Leica).

Lipid Extraction and Analysis

Lipids were extracted by the procedure of Bligh and Dyer (BLIGH and DYER 1959), with minor modifications as described previously by Martin et al. (2005). Aliquots of each lipid extract were used for preparation of fatty acid methyl esters (FAMES) (Martin et al. 2005). The FAMES were analyzed by GC-FID as described in Ford et al. (Ford et al. 2008).

SDS-PAGE and Western Blotting

Proteins were resolved by 10% SDS-PAGE and transferred to nitrocellulose membranes. The blots were washed twice for 10 min with TTBS [20 mM Tris-HCl (pH 7.4), 100 mM NaCl and 0.1% Tween-20] and blocked with either 5% bovine serum albumin or non-fat dry milk powder (Bio-Rad) in TTBS for 1h at room temperature. Blots were then incubated with anti-IR β (1:1000) or anti-opsin (1:10000) or anti-actin (1:1000) for either 1h (opsin and actin) at room temperature or overnight (IR β) at 4 $^{\circ}$ C. Following primary antibody incubations, immunoblots were incubated with HRP-linked secondary antibodies (mouse or rabbit) and developed by ECL according to the manufacturer's instructions.

Statistical Analysis

For cytochemical studies, at least ten fields/image per sample, randomly chosen, were analyzed in each case. Each value represents the average of at least 3 experiments, with 3–4 dishes for each condition \pm SD, unless otherwise indicated. Statistical significance was determined by Student's two-tailed *t*-test.

RESULTS

Location of IR in rod photoreceptor cells

To demonstrate that insulin receptors are present in photoreceptor outer segments, we immunolabeled bovine ROS (containing some attached inner segment) with an anti-IR β antibody. Immunostaining was found in both outer and inner segments (Fig. 1A). Inclusion of the IR β -blocking peptide inhibited the immunoreactivity of IR β (data not shown).

Photoreceptors were identified by the expression of opsin (Fig. 1B). These results provide strong evidence that the insulin receptor is present in rod photoreceptor cells.

Lack of insulin alters the development of photoreceptors in normal rodent retinas

To explore the involvement of the IR in axonal outgrowth, we evaluated the effects of the absence of insulin on the development of normal rodent retinal neurons. For this purpose, wild type rat retina neurons were cultured in media supplemented with or without insulin. Retinal cells isolated from 1–2 day-old rodent retinas and cultured in a chemically-defined medium grew and differentiated giving rise to purified neuronal cultures consisting, at day 7, mainly of amacrine (55–60%) and photoreceptor (35–40%) cells (Politi et al. 1996; Politi et al. 1988). In insulin-supplemented cultures, photoreceptors showed a normal morphology, displaying neurites with narrow axon cones (white arrows in Figs. 2A, C). To further visualize the organization of the actin cytoskeleton in these cultures we stained photoreceptors with phalloidin, which selectively binds to F-actin, and the staining revealed a normal actin cytoskeleton (white arrow in Fig. 2A). On the contrary, photoreceptors developed in insulin-lacking cultures exhibited a widening in their axonal cones and a disruption in their actin cytoskeleton, showing clumps of actin (empty and small arrowheads in Figs. 2D, F).

To investigate whether these changes only affected actin filament organization or whether other cytoskeleton components were also involved, we assessed the expression of tubulin in both insulin supplemented and insulin-lacking cultures (Fig. 3A–F). In insulin-supplemented cultures, photoreceptor axons had a narrow shape that corresponded with a normal tubulin organization (thin arrows in Figs. 3A, C). In the absence of insulin, photoreceptors showed wide axon cones (thin arrows in Figs. 3D, F) and clumps (small arrowheads in Figs. 3D, F), which corresponded with an abnormal tubulin accumulation in the axonal cones and axons. Therefore, the absence of insulin affected both actin and tubulin organization in photoreceptors, suggesting that the IR might regulate the cyto-architecture of the developing neurites.

High glucose and high insulin levels affected normal photoreceptor morphology

To evaluate the effects of high glucose on photoreceptor morphology; neurons were cultured with 25 mM glucose, a concentration 4.5 times higher than controls. This induced actin to lose its filamentous organization (compare Figs. 4A and C), forming clumps in photoreceptor cell bodies and neurites (white arrowheads in Fig. 4C) and sharp pointed spikes that protruded from growth cones and also, though less conspicuous, from the cell body and neurites (Fig. 4C, wide white arrows). Axonal cones showed an abnormal actin distribution, many of them being broader than those in controls. High levels of insulin had a similar effect, producing actin aggregates in the cell body, neurites and axonal cones in photoreceptors (Fig. 4E, white arrowheads) and actin spikes that projected from growth cones (Fig. 4E, wide white arrow).

Docosahexaenoic acid (DHA) prevented abnormal development in photoreceptors

Previous reports have demonstrated that DHA, the major polyunsaturated fatty acid in the retina, prevents apoptosis and promotes differentiation in photoreceptors (Rotstein et al. 1996). We investigated whether DHA prevented the abnormal development of photoreceptors in insulin-lacking cultures. When DHA was added to cultures lacking insulin, photoreceptors developed normal, thin axons (Figs. 2G–I) with no signs of actin (Fig. 2G) or tubulin (Fig. 3G) disorganization. The above results suggest that both DHA and insulin activate signaling mechanisms which lead to axonal outgrowth in photoreceptors.

Effect of insulin and DHA on cytochalasin D disruption of actin cytoskeleton

To further evaluate insulin and DHA protection of the actin cytoskeleton, cells were treated with cytochalasin D, an inhibitor of actin polymerization that disrupts actin microfilaments. In insulin-lacking cultures, cytochalasin D disorganized the actin network; actin concentrated in clumps throughout the cell body, neurites and lamellipodia (Fig. 4G, white arrowheads) and also in axonal cones, some of which showed an increase in width similar to that observed in insulin-lacking cultures. Insulin only slightly prevented cytochalasin D effects, with multiple abnormal actin accumulations being visible in the cell body, lamellipodia and axonal cones (white arrowheads in Fig. 4I). DHA addition to insulin-lacking cultures showed a more effective protection than that of insulin, though axonal and growth cones still showed small actin aggregates (not shown). Combined addition of DHA and insulin effectively protected the actin cytoskeleton (Fig. 4K), preserving an almost normal morphology in axonal cones in spite of cytochalasin D treatment.

Lack of insulin alters axonal outgrowth in amacrine neurons from normal rodent retinas

In insulin-lacking cultures, amacrine neurons develop abnormal neurites and become apoptotic (Politi et al. 2001). We investigated whether organization of their cytoskeleton was also affected in insulin-lacking cultures. As expected, in cultures supplemented with insulin, amacrine neurons developed an extensive neurite outgrowth and showed intact nuclei and a normal actin and tubulin organization (open arrows in Figs. 2A–C, 3A–C). As previously reported, in the absence of insulin, amacrine neurons (open arrows in Figs. 5A–C) developed abnormal, non-branched neurites, which showed tubulin disorganization; in addition, many amacrine neurites showed wide axonal cones (white thin arrows in Figs. 5A, C), resembling those observed in photoreceptors.

Noteworthy, the disorganization of amacrine neurites in insulin-lacking cultures was not prevented by DHA addition; under these conditions amacrine neurons grew extensive lamellipodia (wide, white-filled arrows in Fig. 3G) but were unable to develop their characteristic branched neurites (compare Figs. 3A and 3G). Cytochalasin D produced a loss of actin labeling (compare Figs. 4A and G) and the formation of actin clumps in lamellipodia (Fig. 4G, white arrowheads). Though DHA prevented many of these changes, actin clumps were still visible in amacrine cell lamellipodia, even in insulin-supplemented cultures (not shown). These results suggest that DHA affected axonal development in photoreceptors and in amacrine neurons in a different manner, probably by activating different signaling cascades.

Generation of the conditional IR knockout mice

To determine whether the insulin-induced activation of IR signaling is essential for photoreceptor differentiation, we established retinal cultures from IR knockout mice. Mice lacking IR are born with normal features but develop early postnatal diabetes and die of ketoacidosis (Accili et al. 1996; Joshi et al. 1996). Therefore, a conditional IR disruption strategy was applied by mating rod-expressing Cre mice and floxed IR mice to generate conditional IR knockout mice (Rajala et al. 2008). Though we recently reported reduced levels of IR in rod specific IR knockout mouse retinas (Rajala et al. 2008), in the present study we evaluated IR levels again, since different lines of conditional IR knockout mice can give different levels of recombination (different levels of IR deletion) and to ensure that these animals were true conditional IR knockouts. Figures 6A and B show the genotyping analysis of IR conditional knockout mice. To evaluate the efficiency of deletion of the IR in rod photoreceptors triggered by opsin-driven Cre expression, ROS membranes were prepared from homozygous conditional IR knockout and wild-type mice and subjected to Western blot analysis with anti-IR β , anti-actin, and anti-arrestin antibodies. ROS membranes from IR knockout mice generated with the 0.2 kb opsin-*cre* promoter had 70% less IR

protein content than ROS membranes from control mice (Fig. 6C). In parallel, reduced expression of actin was observed in IR conditional knockout mouse retinas compared to controls (Fig. 6D); however, the expression of arrestin remained the same in both groups (Fig. 6E). Densitometric analysis of immunoblots of actin was performed in the linear range of detection and absolute values were then normalized to photoreceptor specific protein arrestin (F).

Occurrence of abnormal photoreceptors in IR knockout mouse retinal cultures

The changes in photoreceptor cell morphology observed in insulin-lacking cultures (Figs. 2, 3 and 4) suggested the relevance of IR signaling on photoreceptor development. To further corroborate this relevance, we investigated whether photoreceptor development was also affected in IR knockout mice. Photoreceptor cells obtained from wild type mouse (Fig. 7B) and rat retinas (Fig. 2C) were remarkably similar: they displayed a small cell body (3–6 μm) with a single axon, usually bearing a synaptic spherule at its end (Fig. 7B, open arrow). Strikingly, photoreceptor cells from IR knockout mice showed a similarly small cell body but had much wider axonal cones at the beginning of their neurites (thin white arrow, Fig. 7A). Axonal cones in IR knockout mice photoreceptors were almost twice the width of those from wild type mice (Figs. 7A, B). This increase in width was similar and affected a similar amount of photoreceptors in insulin-lacking cultures and IR knockout mice, since the percentage of photoreceptors having wide axonal cones increased from about 20% in control and wild type photoreceptors to over 50% in insulin-lacking and IR knockout photoreceptors (Figs. 7C, D). These results support the hypothesis that the IR might regulate the cyto-architecture of the developing neurites. We then investigated whether these changes were coincident with an abnormal expression of IR in neuronal cultures obtained from IR knockout mouse retinas. In effect, a reduced expression of IR was found in neurons from IR knockout mouse retinas compared to those from wild-type retinas (compare Figs. 7E, F). To confirm the identity of the abnormal retinal neurons in IR knockout mouse retinas as photoreceptors, we stained neurons with an opsin antibody, which evidenced the expression of opsin in these cells (Figs. 7G, H). As a whole, these results suggest that IR deletion may contribute to the abnormal morphological phenotype in rod photoreceptors.

Actin disorganization in the IR knockout mouse retinal neurons

Since actin expression was decreased in IR KO retinas, we investigated whether their abnormal morphology could be due to disruption of the actin cytoskeleton. Phalloidin staining of wild type and IR knockout mice photoreceptors revealed a remarkable disorganization of the actin network in photoreceptors from IR knockout mouse retinas; instead of showing the typical fasciculation of actin, found in photoreceptors from wild type mice (Fig. 7I), the IR knockout photoreceptors showed a conspicuous accumulation of actin filaments, which were concentrated in the periphery of the cell body (small white arrows in Fig. 7J). These results suggest that the IR-activated signaling cascade might regulate the assembly of the actin cytoskeleton in photoreceptor neurons.

Fatty acid levels in light- and dark-adapted ROS membranes

We previously reported that light induces the activation of the retinal IR, and this activation is photoreceptor-specific (Rajala et al. 2002). To determine whether the light-induced activation of IR has any relationship with DHA levels in the light-adapted ROS, we prepared ROS membranes from light- and dark-adapted rats (three independent preparations). Gel Code Blue-stained gels of the ROS prepared from dark- and light-adapted rats are shown in Fig. 8A. Alpha subunit of transducin was used as a positive control for dark-adaptation and arrestin was used as a positive control for light-adaptation; opsin was used as an internal control for both dark- and light-adaptation. There were no obvious differences in the purity of the preparation of ROS from both dark- and light-adapted conditions. Therefore,

differences in the fatty acid composition of ROS membranes between dark- and light-adapted conditions were not the result of contamination of membranes with non-ROS material. Gas chromatography analyses of ROS showed that light-adapted rats had higher amounts (nmoles/ug protein) of DHA as well as total fatty acids than those from dark-adapted rats (Fig. 8B). The relative mole percent of DHA from dark- and light-adapted ROS are 56.25 ± 0.20 and 57.10 ± 0.20 ($p < 0.036$, $n=3$), respectively. The lower nmole/protein level of DHA in the dark-adapted ROS (Fig. 8B) is most likely a reflection of the lower level of total nmole fatty acid/protein.

DISCUSSION

The central observation of this study is that the insulin-lacking cultures, photoreceptors from wild type rat retinas exhibited an abnormal morphology with a wide axon cone and disorganization of the actin and tubulin cytoskeleton. Photoreceptors from IR knockout mouse retinas also exhibited a similar abnormal morphology. A novel finding in this study was that addition of docosahexaenoic acid (DHA), a photoreceptor trophic factor, restored normal axonal outgrowth in insulin-lacking cultures. These data suggest that IR-signaling pathways regulate actin and tubulin cytoskeletal organization in photoreceptors; they also imply that insulin and DHA activate at least partially overlapping signaling pathways that are essential for the development of normal photoreceptors.

It has been recently reported that insulin prevents cone photoreceptor cell death in an animal model of retinitis pigmentosa, suggesting that this phenotype is due to nutrient starvation (Punzo et al. 2009). Insulin has previously been shown to be essential for the survival and development of amacrine neurons, but not for the survival of rod photoreceptors (Politi et al. 2001). The present results demonstrated that deletion of IR or lack of insulin led to the development of abnormal photoreceptor morphology, suggesting that insulin might be an important trophic factor for development of normal photoreceptors.. Consistent with these observations, it has been reported previously that in *Drosophila*, the IR serves an important function to guide retinal photoreceptor axons from the retina to the brain during development (Song et al. 2003) and the IR also influences the size and number of photoreceptors (Brogiolo et al. 2001).

The disorganization of actin cytoskeleton was the detectable phenotype observed in IR-deleted photoreceptors. A reduction in ROS-associated actin (presumably F-actin) was also found in IR knockout mouse retinas compared to wild type mouse retinas. Hence, the occurrence of abnormal axons in IR-deleted photoreceptors and in normal photoreceptors in cultures devoid of insulin might arise from both a deficiency and a disorganization of cytoskeleton structural components. While microtubules are mainly involved in axonal transport, actin filaments contribute to cell morphology, and hence both play a role in the regulation of neurite outgrowth. The tubulin disorganization observed in neurons from the IR knockout mice, and in wild type rodents in the absence of insulin, might interfere with actin transport, resulting in an excessive (abnormal) accumulation of actin filaments in the axonal cones. In turn, this actin accumulation would lead to the development of wide axonal cones, as those observed here.

In muscle cells in culture, insulin induces a rapid actin filament reorganization that coincides with plasma membrane ruffling and intense accumulation of pinocytotic vesicles (Tsakiridis et al. 1999). Initiation of these effects of insulin requires an intact actin cytoskeleton and activation of PI3K (Tsakiridis et al. 1999). These observations suggest that the actin cytoskeleton facilitates propagation of the morphological, metabolic, and nuclear effects of insulin by regulating proper subcellular distribution of signaling molecules that participate in the insulin signaling pathway. Phosphoinositides are the key molecules for regulation of

actin cytoskeletal organization and membrane traffic from the plasma membrane (Takenawa and Itoh 2001). In photoreceptors, we previously reported that the IR regulates PI3K and Akt activation (Rajala et al. 2007; Rajala et al. 2008; Rajala et al. 2002). Further, we recently reported that 3'-phosphoinositides generated through light-induced tyrosine phosphorylation of IR regulates the reorganization of actin cytoskeleton (Li et al. 2008). The results from our current study also suggest that IR activation may regulate the actin cytoskeletal organization. Dysfunction of the actin cytoskeleton is a key event in the pathogenesis of diabetic nephropathy (Conway et al. 2004), diabetic neuropathy (McLean 1997; McLean et al. 1995) and diabetic cardiomyopathy (Olson et al. 1998; Fein et al. 1984). Our findings that high glucose and high insulin concentrations induced severe morphological changes in actin cytoskeleton, altering growth cone structure, are consistent with reports showing impaired axonal growth and aberrant dystrophic structures in dorsal root ganglion neurons from diabetic animals and in neurons cultured under high glucose conditions (Zherebitskaya et al. 2009; Tosaki et al. 2008). *In vitro* and *in vivo* evidence for a bidirectionally causal relationship between chronic exposure to hyperinsulinemia and insulin resistance through desensitization of insulin signaling pathway has been reported. Examples include, 24 hour incubation of L6-myoblasts with high insulin levels induces a PI3K-mediated reduction in IR substrate protein (IRS-1) expression and desensitization of insulin signaling pathway (Del Prato et al. 1994; Bertacca et al. 2005; Pirola et al. 2004). Continuation of exposure of cultured myoblasts to high insulin is associated with a demodulation of IR signaling through down regulation of IR, IRS-1, PI3K and Akt activity (Huang et al. 2002). Chronic hyperinsulinemic rats have insulin resistance accompanied by impairment of insulin-induced IR/IRSs/PI3K/Akt pathway in liver and muscle (Hirashima et al. 2003). The IR-activated PI3K-generated phosphoinositides in the retina might play an important role in the control of diabetic retinopathy. Further studies are required to examine whether the photoreceptor-specific IR knockout mice are more susceptible to diabetic retinopathy.

DHA promotes the survival and differentiation of photoreceptors by activating the ERK/MAP kinase pathway (Rotstein et al. 1996; Rotstein et al. 1998; German et al. 2006) and stimulating axonal outgrowth in these neurons (Garelli et al. 2006). It has also been shown to increase neurite outgrowth in hippocampal neurons and in human neuroblastoma cells (Calderon and Kim 2004; Wu et al. 2009), its oral administration augmenting dendritic spine density and actin levels in gerbil hippocampus (Sakamoto et al. 2007). Our results show that DHA prevented the abnormal axonal development of photoreceptors induced by insulin depletion. Moreover, when the actin cytoskeleton was disorganized using cytochalasin D, DHA, and, to a much lesser extent, insulin, preserved the actin network in growth and axonal cones, the combined addition of both molecules providing the most effective protection. These results suggest that insulin and DHA are involved in the stabilization of the actin fibers and, consequently, in the preservation of cell and axon morphology, though by activating pathways that might either be different or partially overlap.

We previously reported that light induces the activation of retinal IR and its downstream effector molecules, PI3K and Akt, in ROS membranes (Rajala et al. 2007; Li et al. 2008). We suspect that this activation could be due to changes in DHA levels in the ROS membranes. Consistent with this hypothesis, we observed higher amounts of DHA in light-adapted ROS membranes. In this study we did not observe any DHA-induced direct activation of IR *in vitro* (data not shown); however, DHA may indirectly be activating the IR signal transduction pathway. DHA has shown to be a positive modulator of Akt signaling in neuronal cells (Akbar et al. 2005). These authors have also shown that DHA has no effect on PI3K activity. Based on our current studies, along with the previously published work on DHA and Akt, we propose that insulin receptor signaling is important for the development

of normal photoreceptors and the activated pathways could be either insulin-PI3K-Akt or DHA-Akt.

As a whole, our present results suggest that multiple trophic factors, among them insulin and DHA, activate different signaling pathways to control actin cytoskeleton in developing photoreceptors and axonal outgrowth. The finding that DHA prevented the abnormal development of photoreceptor axons in insulin-depleted cultures suggests that insulin and DHA may at times play coincident and overlapping roles in activating signaling cascades to control key aspects of photoreceptor development.

Acknowledgments

This work was supported by grants from the National Institutes of Health (EY016507; EY00871), NEI Core grant (EY12190), NCCR COBRE core modules (P20-RR17703) and Research to Prevent Blindness Inc. We are thankful to EB de los Santos, from the Instituto de Investigaciones Bioquímicas de Bahía Blanca, for excellent technical assistance.

ABBREVIATIONS

IR	insulin receptor
PI3K	phosphoinositide 3-kinase
IRβ	IR beta subunit
ROS	rod outer segments
DHA	docosahexaenoic acid

References

- Accili D, Drago J, Lee EJ, Johnson MD, Cool MH, Salvatore P, Asico LD, Jose PA, Taylor SI, Westphal H. Early neonatal death in mice homozygous for a null allele of the insulin receptor gene. *Nat Genet.* 1996; 12:106–109. [PubMed: 8528241]
- Adler R. Regulation of neurite growth in purified retina neuronal cultures: effects of PNPf, a substratum-bound, neurite-promoting factor. *J Neurosci Res.* 1982; 8:165–177. [PubMed: 6897553]
- Akbar M, Calderon F, Wen Z, Kim HY. Docosahexaenoic acid: a positive modulator of Akt signaling in neuronal survival. *Proc Natl Acad Sci U S A.* 2005; 102:10858–10863. [PubMed: 16040805]
- Barber AJ, Nakamura M, Wolpert EB, Reiter CE, Seigel GM, Antonetti DA, Gardner TW. Insulin rescues retinal neurons from apoptosis by a phosphatidylinositol 3-kinase/Akt-mediated mechanism that reduces the activation of caspase-3. *J Biol Chem.* 2001; 276:32814–32821. [PubMed: 11443130]
- Baskin DG, Figlewicz LD, Seeley RJ, Woods SC, Porte D Jr, Schwartz MW. Insulin and leptin: dual adiposity signals to the brain for the regulation of food intake and body weight. *Brain Res.* 1999; 848:114–123. [PubMed: 10612703]
- Bertacca A, Ciccarone A, Cecchetti P, Vianello B, Laurenza I, Maffei M, Chiellini C, Del Prato S, Benzi L. Continually high insulin levels impair Akt phosphorylation and glucose transport in human myoblasts. *Metabolism.* 2005; 54:1687–1693. [PubMed: 16311104]
- BLIGH EG, DYER WJ. A rapid method of total lipid extraction and purification. *Can J Biochem Physiol.* 1959; 37:911–917. [PubMed: 13671378]
- Brogio W, Stocker H, Ikeya T, Rintelen F, Fernandez R, Hafen E. An evolutionarily conserved function of the Drosophila insulin receptor and insulin-like peptides in growth control. *Curr Biol.* 2001; 11:213–221. [PubMed: 11250149]
- Calderon F, Kim HY. Docosahexaenoic acid promotes neurite growth in hippocampal neurons. *J Neurochem.* 2004; 90:979–988. [PubMed: 15287904]

- Conway BR, Maxwell AP, Savage DA, Patterson CC, Doran PP, Murphy M, Brady HR, Fogarty DG. Association between variation in the actin-binding gene caldesmon and diabetic nephropathy in type 1 diabetes. *Diabetes*. 2004; 53:1162–1165. [PubMed: 15047636]
- Del Prato S, Leonetti F, Simonson DC, Sheehan P, Matsuda M, DeFronzo RA. Effect of sustained physiologic hyperinsulinaemia and hyperglycaemia on insulin secretion and insulin sensitivity in man. *Diabetologia*. 1994; 37:1025–1035. [PubMed: 7851681]
- Fein FS, Malhotra A, Miller-Green B, Scheuer J, Sonnenblick EH. Diabetic cardiomyopathy in rats: mechanical and biochemical response to different insulin doses. *Am J Physiol*. 1984; 247:H817–H823. [PubMed: 6238541]
- Ford DA, Monda JK, Brush RS, Anderson RE, Richards MJ, Fliesler SJ. Lipidomic analysis of the retina in a rat model of Smith-Lemli-Opitz syndrome: alterations in docosahexaenoic acid content of phospholipid molecular species. *J Neurochem*. 2008; 105:1032–1047. [PubMed: 18182048]
- Frolich L, Blum-Degen D, Bernstein HG, Engelsberger S, Humrich J, Laufer S, Muschner D, Thalheimer A, Turk A, Hoyer S, Zochling R, Boissl KW, Jellinger K, Riederer P. Brain insulin and insulin receptors in aging and sporadic Alzheimer's disease. *J Neural Transm*. 1998; 105:423–438. [PubMed: 9720972]
- Garelli A, Rotstein NP, Politi LE. Docosahexaenoic acid promotes photoreceptor differentiation without altering Crx expression. *Invest Ophthalmol Vis Sci*. 2006; 47:3017–3027. [PubMed: 16799048]
- German OL, Insua MF, Gentili C, Rotstein NP, Politi LE. Docosahexaenoic acid prevents apoptosis of retina photoreceptors by activating the ERK/MAPK pathway. *J Neurochem*. 2006; 98:1507–1520. [PubMed: 16923163]
- Havrankova J, Roth J, Brownstein M. Insulin receptors are widely distributed in the central nervous system of the rat. *Nature*. 1978; 272:827–829. [PubMed: 205798]
- Heidenreich KA. Insulin and IGF-I receptor signaling in cultured neurons. *Ann N Y Acad Sci*. 1993; 692:72–88. [PubMed: 8215046]
- Hirashima Y, Tsuruzoe K, Kodama S, Igata M, Toyonaga T, Ueki K, Kahn CR, Araki E. Insulin down-regulates insulin receptor substrate-2 expression through the phosphatidylinositol 3-kinase/Akt pathway. *J Endocrinol*. 2003; 179:253–266. [PubMed: 14596677]
- Huang C, Somwar R, Patel N, Niu W, Torok D, Klip A. Sustained exposure of L6 myotubes to high glucose and insulin decreases insulin-stimulated GLUT4 translocation but upregulates GLUT4 activity. *Diabetes*. 2002; 51:2090–2098. [PubMed: 12086937]
- Joshi RL, Lamothe B, Cordonnier N, Mesbah K, Monthieux E, Jami J, Bucchini D. Targeted disruption of the insulin receptor gene in the mouse results in neonatal lethality. *EMBO J*. 1996; 15:1542–1547. [PubMed: 8612577]
- Li G, Anderson RE, Tomita H, Adler R, Liu X, Zack DJ, Rajala RV. Nonredundant role of Akt2 for neuroprotection of rod photoreceptor cells from light-induced cell death. *J Neurosci*. 2007; 27:203–211. [PubMed: 17202487]
- Li G, Rajala A, Wiechmann AF, Anderson RE, Rajala RV. Activation and membrane binding of retinal protein kinase Balpha/Akt1 is regulated through light-dependent generation of phosphoinositides. *J Neurochem*. 2008; 107:1382–1397. [PubMed: 18823366]
- Martin RE, Elliott MH, Brush RS, Anderson RE. Detailed characterization of the lipid composition of detergent-resistant membranes from photoreceptor rod outer segment membranes. *Invest Ophthalmol Vis Sci*. 2005; 46:1147–1154. [PubMed: 15790872]
- McLean WG. The role of axonal cytoskeleton in diabetic neuropathy. *Neurochem Res*. 1997; 22:951–956. [PubMed: 9239750]
- McLean WG, Roberts RE, Mullins FH. Post-translational modifications of microtubule- and growth-associated proteins in nerve regeneration and neuropathy. *Biochem Soc Trans*. 1995; 23:76–80. [PubMed: 7758794]
- Muresan V, Joshi HC, Besharse JC. Gamma-tubulin in differentiated cell types: localization in the vicinity of basal bodies in retinal photoreceptors and ciliated epithelia. *J Cell Sci*. 1993; 104 (Pt 4): 1229–1237. [PubMed: 7686172]

- Olson TM, Michels VV, Thibodeau SN, Tai YS, Keating MT. Actin mutations in dilated cardiomyopathy, a heritable form of heart failure. *Science*. 1998; 280:750–752. [PubMed: 9563954]
- Pirola L, Johnston AM, Van Obberghen E. Modulation of insulin action. *Diabetologia*. 2004; 47:170–184. [PubMed: 14722654]
- Politi LE, Bouzat C, los Santos EB, Barrantes FJ. Heterologous retinal cultured neurons and cell adhesion molecules induce clustering of acetylcholine receptors and polynucleation in mouse muscle BC3H-1 clonal cell line. *J Neurosci Res*. 1996; 43:639–651. [PubMed: 8984194]
- Politi LE, Lehar M, Adler R. Development of neonatal mouse retinal neurons and photoreceptors in low density cell culture. *Invest Ophthalmol Vis Sci*. 1988; 29:534–543. [PubMed: 3281914]
- Politi LE, Rotstein NP, Salvador G, Giusto NM, Insua MF. Insulin-like growth factor-I is a potential trophic factor for amacrine cells. *J Neurochem*. 2001; 76:1199–1211. [PubMed: 11181839]
- Punzo C, Kornacker K, Cepko CL. Stimulation of the insulin/mTOR pathway delays cone death in a mouse model of retinitis pigmentosa. *Nat Neurosci*. 2009; 12:44–52. [PubMed: 19060896]
- Rajala A, Anderson RE, Ma JX, Lem J, Al Ubaidi MR, Rajala RV. G-protein-coupled Receptor Rhodopsin Regulates the Phosphorylation of Retinal Insulin Receptor. *J Biol Chem*. 2007; 282:9865–9873. [PubMed: 17272282]
- Rajala A, Tanito M, Le YZ, Kahn CR, Rajala RV. Loss of neuroprotective survival signal in mice lacking insulin receptor gene in rod photoreceptor cells. *J Biol Chem*. 2008; 283:19781–19792. [PubMed: 18480052]
- Rajala RV, McClellan ME, Ash JD, Anderson RE. In vivo regulation of phosphoinositide 3-kinase in retina through light-induced tyrosine phosphorylation of the insulin receptor beta-subunit. *J Biol Chem*. 2002; 277:43319–43326. [PubMed: 12213821]
- Reiter CE, Wu X, Sandirasegarane L, Nakamura M, Gilbert KA, Singh RS, Fort PE, Antonetti DA, Gardner TW. Diabetes reduces basal retinal insulin receptor signaling: reversal with systemic and local insulin. *Diabetes*. 2006; 55:1148–1156. [PubMed: 16567541]
- Robinson LJ, Leitner W, Draznin B, Heidenreich KA. Evidence that p21ras mediates the neurotrophic effects of insulin and insulin-like growth factor I in chick forebrain neurons. *Endocrinology*. 1994; 135:2568–2573. [PubMed: 7988444]
- Rotstein NP, Avelldano MI, Barrantes FJ, Politi LE. Docosahexaenoic acid is required for the survival of rat retinal photoreceptors in vitro. *J Neurochem*. 1996; 66:1851–1859. [PubMed: 8780010]
- Rotstein NP, Avelldano MI, Barrantes FJ, Roccamo AM, Politi LE. Apoptosis of retinal photoreceptors during development in vitro: protective effect of docosahexaenoic acid. *J Neurochem*. 1997; 69:504–513. [PubMed: 9231708]
- Rotstein NP, Politi LE, Avelldano MI. Docosahexaenoic acid promotes differentiation of developing photoreceptors in culture. *Invest Ophthalmol Vis Sci*. 1998; 39:2750–2758. [PubMed: 9856786]
- Sakamoto T, Cansev M, Wurtman RJ. Oral supplementation with docosahexaenoic acid and uridine-5'-monophosphate increases dendritic spine density in adult gerbil hippocampus. *Brain Res*. 2007; 1182:50–59. [PubMed: 17950710]
- Schubert M, Gautam D, Surjo D, Ueki K, Baudler S, Schubert D, Kondo T, Alber J, Galldiks N, Kustermann E, Arndt S, Jacobs AH, Krone W, Kahn CR, Bruning JC. Role for neuronal insulin resistance in neurodegenerative diseases. *Proc Natl Acad Sci U S A*. 2004; 101:3100–3105. [PubMed: 14981233]
- Schwartz MW, Sipols AJ, Marks JL, Sanacora G, White JD, Scheurink A, Kahn SE, Baskin DG, Woods SC, Figlewicz DP. Inhibition of hypothalamic neuropeptide Y gene expression by insulin. *Endocrinology*. 1992; 130:3608–3616. [PubMed: 1597158]
- Song J, Wu L, Chen Z, Kohanski RA, Pick L. Axons guided by insulin receptor in *Drosophila* visual system. *Science*. 2003; 300:502–505. [PubMed: 12702880]
- Takahashi M, Yamada T, Tooyama I, Moroo I, Kimura H, Yamamoto T, Okada H. Insulin receptor mRNA in the substantia nigra in Parkinson's disease. *Neurosci Lett*. 1996; 204:201–204. [PubMed: 8938265]
- Takenawa T, Itoh T. Phosphoinositides, key molecules for regulation of actin cytoskeletal organization and membrane traffic from the plasma membrane. *Biochim Biophys Acta*. 2001; 1533:190–206. [PubMed: 11731330]

- Tosaki T, Kamiya H, Yasuda Y, Naruse K, Kato K, Kozakae M, Nakamura N, Shibata T, Hamada Y, Nakashima E, Oiso Y, Nakamura J. Reduced NGF secretion by Schwann cells under the high glucose condition decreases neurite outgrowth of DRG neurons. *Exp Neurol*. 2008; 213:381–387. [PubMed: 18675804]
- Tsakiridis T, Tong P, Matthews B, Tsiani E, Bilan PJ, Klip A, Downey GP. Role of the actin cytoskeleton in insulin action. *Microsc Res Tech*. 1999; 47:79–92. [PubMed: 10523787]
- Wolkow CA, Kimura KD, Lee MS, Ruvkun G. Regulation of *C. elegans* life-span by insulinlike signaling in the nervous system. *Science*. 2000; 290:147–150. [PubMed: 11021802]
- Wu H, Ichikawa S, Tani C, Zhu B, Tada M, Shimoishi Y, Murata Y, Nakamura Y. Docosahexaenoic acid induces ERK1/2 activation and neurogenesis via intracellular reactive oxygen species production in human neuroblastoma SH-SY5Y cells. *Biochim Biophys Acta*. 2009; 1791:8–16. [PubMed: 18996496]
- Yi X, Schubert M, Peachey NS, Suzuma K, Burks DJ, Kushner JA, Suzuma I, Cahill C, Flint CL, Dow MA, Leshan RL, King GL, White MF. Insulin receptor substrate 2 is essential for maturation and survival of photoreceptor cells. *J Neurosci*. 2005; 25:1240–1248. [PubMed: 15689562]
- Yu X, Rajala RV, McGinnis JF, Li F, Anderson RE, Yan X, Li S, Elias RV, Knapp RR, Zhou X, Cao W. Involvement of insulin/phosphoinositide 3-kinase/Akt signal pathway in 17 beta-estradiol-mediated neuroprotection. *J Biol Chem*. 2004; 279:13086–13094. [PubMed: 14711819]
- Zheng L, Anderson RE, Agbaga MP, Rucker EB III, Le YZ. Loss of BCL-XL in Rod Photoreceptors: Increased Susceptibility to Bright Light Stress. *Invest Ophthalmol Vis Sci*. 2006; 47:5583–5589. [PubMed: 17122152]
- Zherebitskaya E, Akude E, Smith DR, Fernyhough P. Development of selective axonopathy in adult sensory neurons isolated from diabetic rats: role of glucose-induced oxidative stress. *Diabetes*. 2009; 58:1356–1364. [PubMed: 19252136]

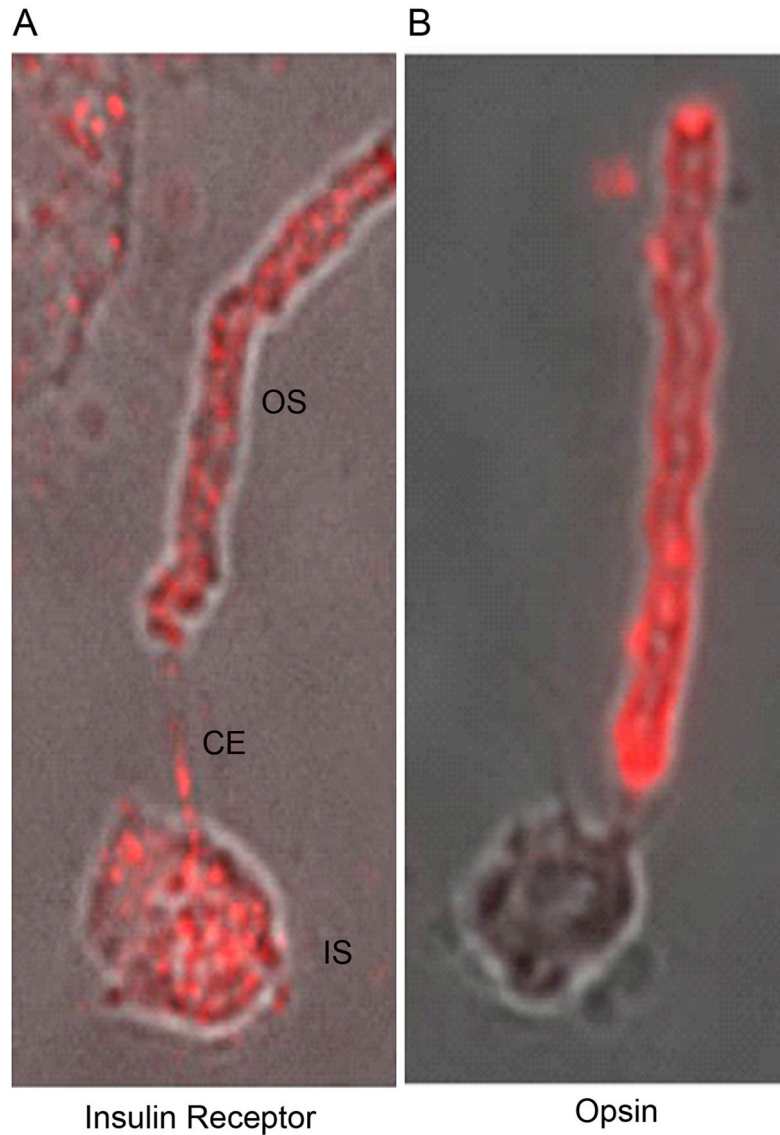


Figure 1. Immunolocalization of IR β in dissociated ROS. Bovine ROS were prepared on glass slides as described in the “Materials and Methods” section. Immunolabeling with IR β (A) and opsin (B). Opsin labeling was used to identify rod photoreceptors. The localization of IR β (A) clearly demonstrates the presence of IR β in rod photoreceptors. OS, outer segments; CE, connecting cilium; IS, inner segment.

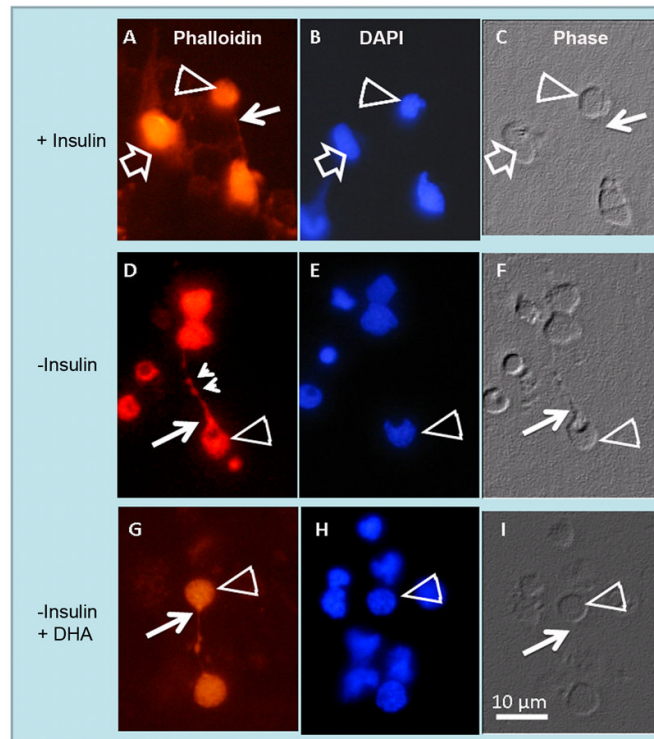


Figure 2.

Abnormal axonal development in insulin-lacking photoreceptors. Rat retina amacrine (open arrows) and photoreceptor (open arrowheads) neurons were cultured with (A, B, C) or without (D, E, F) insulin, or without insulin and with 6.7 μM docosahexaenoic acid (DHA) (G, H, I) for 6 days. Phase (C, F, I) and fluorescence photomicrographs showing DAPI (B, E, H) and actin labeling with rhodamine phalloidin (A, D, G). In the presence of insulin (A–C) photoreceptor axons showed narrow “axon cones” (white arrows), while in the absence of insulin (D–F) many photoreceptors developed wide axon cones (white arrows) and showed clumps of actin in their cell body (open arrowhead) and neurite (small arrowheads). DHA addition to insulin-lacking cultures (G–I) prevented the abnormal development of photoreceptor axon cones. Note that in insulin-supplemented cultures, amacrine neurons (open arrows in A–C) developed an extensive neurite outgrowth.

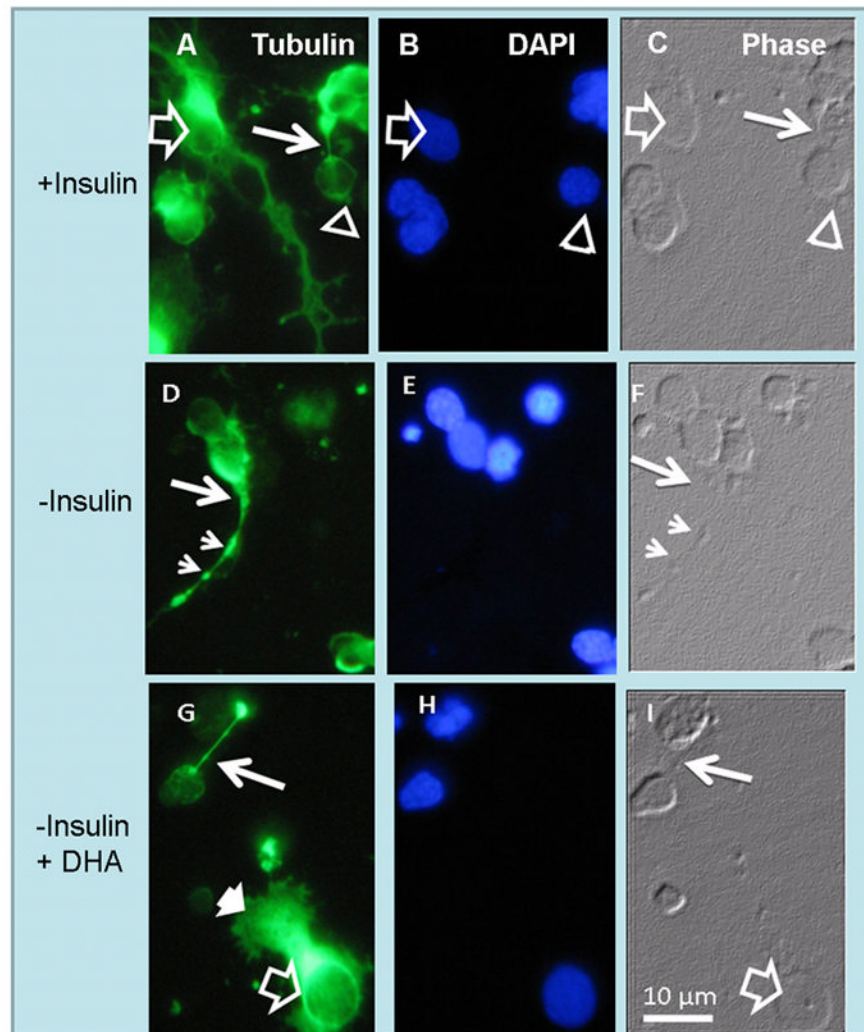


Figure 3.

Anomalous development of axon cones in insulin-lacking photoreceptors. Phase (C, F, I) and fluorescence photomicrographs showing tubulin labeling (A, D, G) and nuclei (B, E, H) of amacrine neurons (open arrows) and photoreceptor (open arrowheads) in day 6 cultures. In the presence of insulin (A–C) photoreceptor axons showed normal “axon cones” (thin white arrows in A, C). Note the extensive neurite outgrowth in amacrine neurons (open arrows in A). Also note that in the absence of insulin (D–F) many photoreceptors developed wide axon cones (thin white arrows) and showed axons with scattered tubulin clumps (small arrowheads in D, F). DHA addition to insulin-lacking cultures (G–I) prevented the abnormal development of photoreceptor axon cones and allowed formation of lamellipodia (white arrowhead in G) in amacrine neurons, but could not reverse their lack of neurite outgrowth.

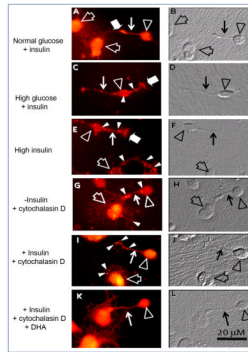


Figure 4.

Effects of high glucose, high insulin and cytochalasin D on actin cytoskeleton in photoreceptors. Phase (B, D, F, H, J, L) and fluorescence (A, C, E, G, I, K) photomicrographs, showing actin labeling of 3 day neuronal cultures in control conditions (A, B, 5.5 mM glucose, 1.66 μ M insulin), with high glucose (C, D, 25 mM glucose, 1.66 μ M insulin) or with high insulin (E, F, 5.5 mM glucose, 16.6 μ M insulin) and of cultures without (G, H) and with (I, J) insulin or with insulin and DHA (K, L), treated at day 3 with 2 μ M cytochalasin D for 30 min. In controls (A, B), photoreceptors (open arrowheads) and amacrine neurons (open arrows) showed a uniform, filamentous actin labeling in neurites (thin white arrows) and cell bodies. High glucose and high insulin led to the formation of actin clumps in photoreceptor cell bodies, axon cones and neurites (white arrowheads in C, E) and of actin spikes that protruded from growth cones (wide white arrows in C, E). In insulin-lacking cultures (G), cytochalasin D disorganized the actin network, with actin clumps being visible in photoreceptor neurites and cell bodies and in amacrine neuron lamellipodia (white arrowheads in G); the loss of actin staining is clearly observed in amacrine lamellipodia (open arrow in G). Insulin slightly prevented cytochalasin effects, though actin clumps were still evident (white arrowheads in I). The combined addition of DHA and insulin preserved a normal actin cytoskeleton in photoreceptor cell bodies and neurites (thin white arrow in K).

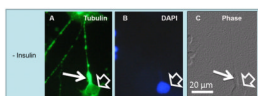


Figure 5. Abnormal development of axon cone development in amacrine neurons growing in insulin-lacking medium. Phase (C) and fluorescence (A, B) photomicrographs showing tubulin (A) and nuclei (B) labeling in day 6 neuronal cultures. In the absence of insulin many amacrine neurons (open arrows) developed wide axon cones (thin white arrows) and tubulin clumps in their neurites, as occurred with photoreceptors.

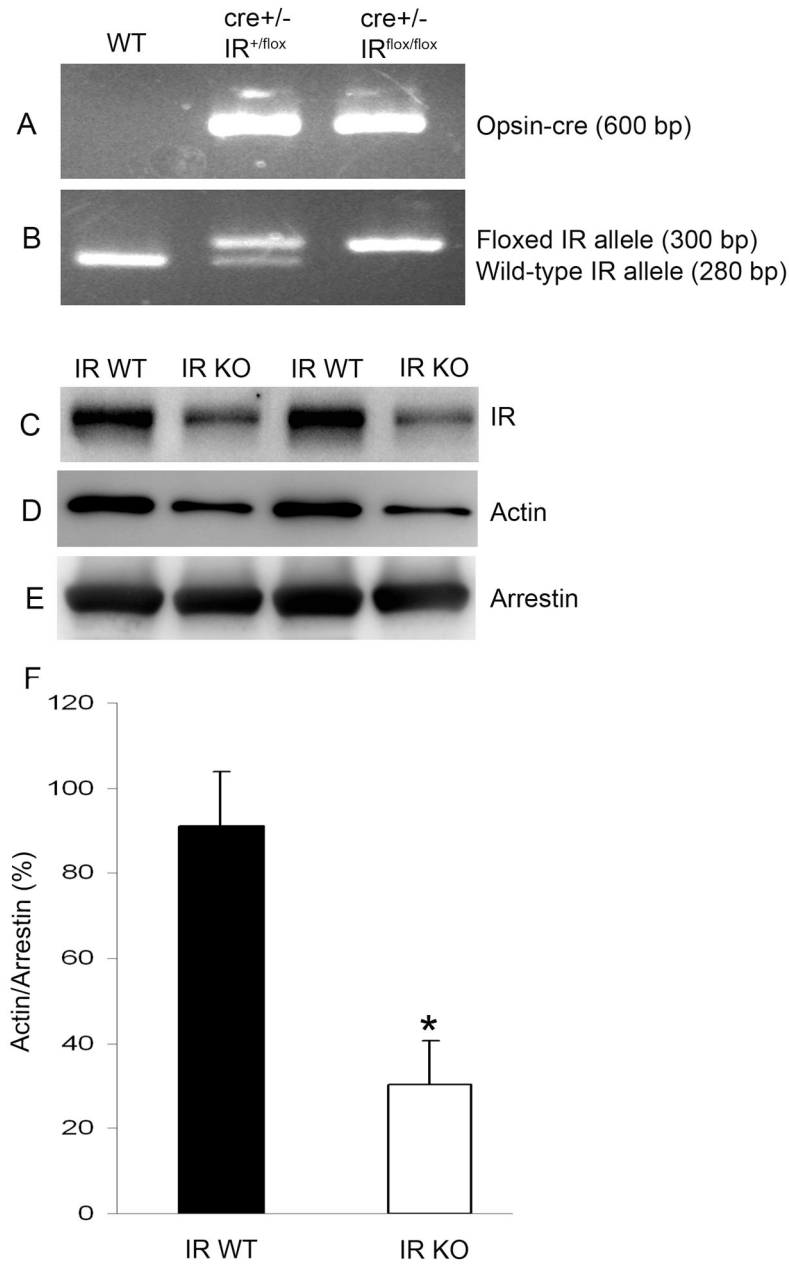


Figure 6. Genotyping of generated photoreceptor-specific IR knockout mice. PCR diagnostic for opsin *cre* (A), and floxed IR and WT genes (B) using mouse tail DNA samples. Rod outer segments (ROS) were prepared from homozygous IR knockout and wild type mice. Equal amounts of ROS were analyzed by Western blot with anti-IR β (C), anti-actin (D), or anti-arrestin (E) antibodies. Quantitative analysis of bands of respective Western blot analyses was performed using Kodak Image Software. Densitometric analysis of immunoblots of actin was performed in the linear range of detection and absolute values were then normalized to photoreceptor specific protein arrestin (F). Data are mean \pm SD. The wild-type control was set as 100 percent. *Statistical significance was determined by Student's two-tailed *t-test* ($p < 0.05$).

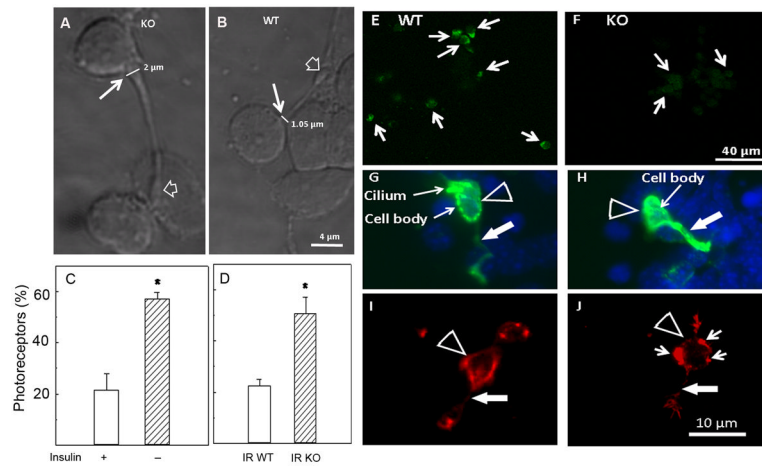


Figure 7.

Abnormal development and differentiation of retina photoreceptors from IR knockout mice. Confocal Nomarsky micrographs of retina photoreceptors from IR deleted (A) and wild type (B) mouse retinas grown in serum-free-chemically defined media for 5 days, showing the increase in width of axonal cones (thin arrow in A, B) from 1.05 μm in WT to 2 μm in KO. Percentage of photoreceptors having wider axonal cones in cultures with (+) or without (-) insulin (C) and in cultures obtained from wild-type (IR WT) or knockout (IR KO) mice retinas (D). Confocal fluorescence micrographs of cultures from wild type (E, G, I) and knockout retinas (F, H, J) were labeled with an antibody against IR β (green staining in E, F), and fluorescence micrographs of cultures double-labeled with DAPI (blue staining) and an anti-opsin antibody (G, H) or with rhodamine phalloidin (red staining in I, J) to examine the organization of F-actin. Photoreceptors of wild type and IR deleted mice showed intense opsin labeling (G, H), even in their neurites (white arrows). Note that in the wild type cultures, IR β occurrence was conspicuous (E), while in IR-deleted cultures it was barely visible (F). Also note the abnormal accumulation of phalloidin in the cell body (short arrows in J) and neurite (white arrow in J) of IR-deleted photoreceptors. Statistical significance was determined by Student's two-tailed *t-test*. *Statistical significant differences compared to controls ($p < 0.05$).

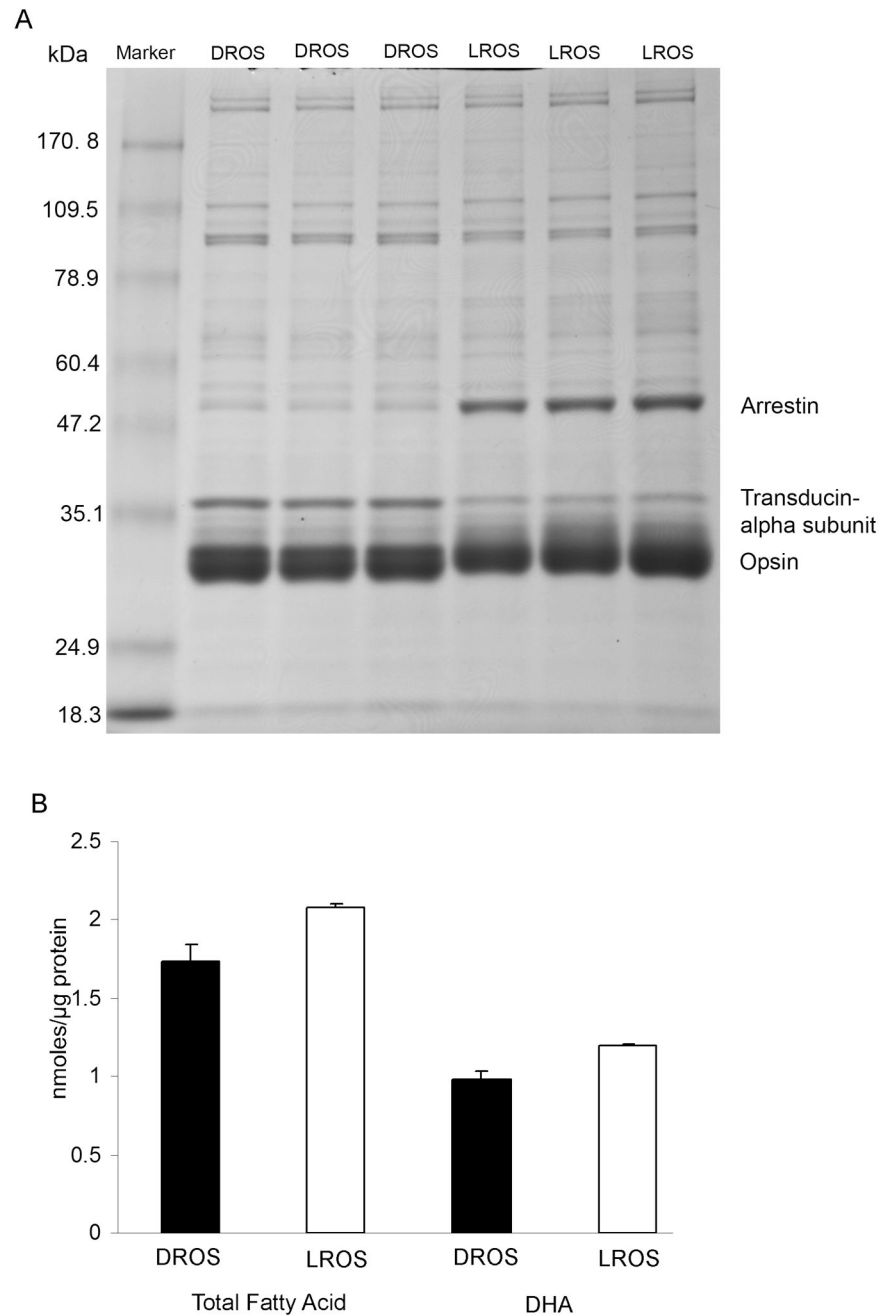


Figure 8. SDS-PAGE and fatty acid analysis on retinas from dark- and light-adapted rats. Representative Gel Code Blue-stained polyacrylamide gels of the dark-(DROS) and light-adapted (LROS) ROS from three independent preparations (8 rats per group). Five micrograms of dark- and light-adapted ROS were subjected to electrophoresis followed by Gel Code Blue stain (A). Total fatty acid and DHA levels (B) were measured in dark- and light-adapted ROS and expressed as nmole FA/μg protein. Data are mean + SD, n=3. Student t test was used to assess the significance between DROS and LROS. Total fatty acid $p < 0.024$; DHA $p < 0.021$.